



# Antibacterial activity of LaNiO<sub>3</sub> prepared by sonicated sol-gel method using combination fuel

Ashwini Lalaso Jadhav<sup>1</sup> · Sanjay Mahadev Khetre<sup>1</sup>

Received: 12 April 2019 / Accepted: 24 October 2019 / Published online: 11 November 2019  
© The Author(s) 2019

## Abstract

Sonicated sol-gel method was used to prepare LaNiO<sub>3</sub> from lanthanum nitrate hexahydrate La(NO<sub>3</sub>)<sub>3</sub>·6H<sub>2</sub>O(LN), nickel nitrate Ni(NO<sub>3</sub>)<sub>2</sub>·6H<sub>2</sub>O(NN), glycine and urea. Nanocrystalline LaNiO<sub>3</sub> powder was formed after heating at 175 °C in 5 min. Particle size of LaNiO<sub>3</sub> nanopowder was determined by Debye Scherrer's equation and was found 48 nm. Prepared nanocatalyst characterized with the help of XRD, TGA, SEM, IR, BET surface area, EDX. Surface area of LaNiO<sub>3</sub> was 9.22 m<sup>2</sup>/g. We have reported first time good antibacterial activity of LaNiO<sub>3</sub> for *Staphylococcus aureus*. Zone of inhibition for LaNiO<sub>3</sub> was 13 mm studied with the help of agar cup method.

**Keywords** Sonicated sol-gel method · LaNiO<sub>3</sub> · EDX · XRD · SEM · Surface area · Antibacterial activity of LaNiO<sub>3</sub>

## Introduction

Over the past few years different nanosized metal oxides are used as antibacterial agents. Metal oxides show antimicrobial activity without causing toxic effect on mammalian cell. Different metal oxides are used as antimicrobial agents. Nanosized HgO antibacterial activity against *Escherichia coli* [1] silver nanoparticles (AgNPs) inhibits growth of bacteria and shows wound-healing properties [2]. Different metal oxides show antibacterial activity effectively against different gram positive and gram negative bacteria. We had studied antibacterial activity of rhombohedral LaNiO<sub>3</sub> against different bacteria and fungi like *E. coli*, *Staphylococcus aureus*, *Streptococcus* spp., *Pseudomonas aeruginosa*, *Bacillus subtilis* and *Candida albicans*. *S. aureus* is a gram positive bacteria that cause different types of infections.

Different strains of *S. aureus* able to secrete different enzymes and bring different antibiotic resistance to groups which increases its pathogenic ability [3]. It shows co-evolution with human hosts. This parasitic co-evolution

with human hosts led to the bacterium ability to be carried in nasopharynx of humans without causing any type of symptoms or infection. Because of which they are passed through human population. Therefore fitness of them as species goes on increasing [4] *S. aureus* shows skin infections, food poisoning, cellulitis, bone and joint infections, bacteremia (bloodstream infection), animal infections in cats, horses, dogs, chickens, and cows. They were found in the form of biofilm [5]. Biofilm matrix protect embedded cells from antibiotic penetration. They show high resistance to host immune response [6]. Genetic element in *S. aureus* includes bacteriophages, pathogenicity island, plasmids, transposons, staphylococcal cassette chromosomes that enable them to show continually evolve and gain new traits which is resistant to antibiotic treatments and host immune response. Because of which there is great genetic variation observed within the *S. aureus*. Different species of *S. aureus* are observed, out of which few show infection in human beings (Fig. 1).

Nanomaterials are today's important scientific concern due to their unique properties and possible application. Mostly ABO<sub>3</sub> is general formula for mixed metal oxide with rhombohedral type structure where 'A' is rare earth alkaline and alkali metal ion that fit into dodecahedral site of framework and B is 3d, 4d transitional metal ion with octahedral site [7, 8].

Recently various mixed rhombohedral metal oxide nanomaterials have been reported [9] with improved catalytic activity and

✉ Ashwini Lalaso Jadhav  
aashwinijadhav321@gmail.com

Sanjay Mahadev Khetre  
sanjaykhetre@gmail.com

<sup>1</sup> Department of Chemistry, Dahiwadi College Dahiwadi,  
Affiliated to Shivaji University, Kolhapur, Tal. Man, Dist.  
Satara, Maharashtra 415508, India



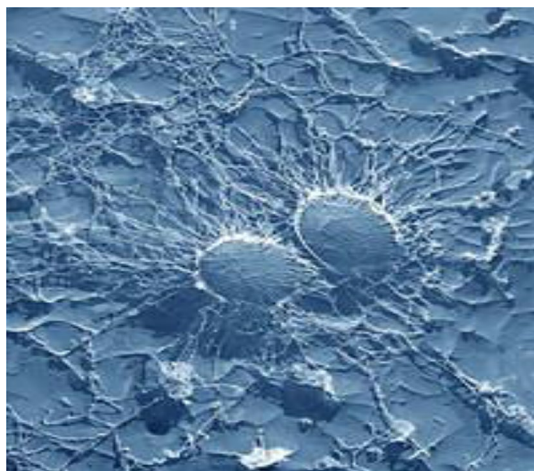


**Fig. 1** Image of *Staphylococcus aureus* bacteria

possibility of use in fuel cells [10]. Various methods like sol-gel [11], co-precipitation [12], liquid mix technique [13], decomposition of mixed oxalate [14], nitrates or carbonates, [15] metallo-organic metallo-inorganic precursors are used to prepare  $\text{LaNiO}_3$ .

Sol-gel method is simple process for production of advance material using heat energy by exothermic reaction. Large quantity of mixed metal oxides synthesized by sol-gel method, because of its simple way, short time, low cost and use of simple equipments. Problem of rapid catalytic deactivation is overcome by rhombohedral material due to its well-defined structure which produces highly dispersed metallic particles to promote high activity suppresses coke formation and enhance catalytic stability. [16–20] Mixed metal oxide nanoparticles used for purification of volatile organic compound (Vocs), total combustion of hydrocarbon for energetic conversion, conducting polymers nanocomposites [21], reduction of  $\text{NO}_x$  and automotive emission, photocatalytic degradation of different dyes [22]. Presently various methods are used to synthesis mixed metal oxide like lanthanum nickel oxide due to its vast application in different fields [23–25].

In present work  $\text{LaNiO}_3$  was prepared using sonicated sol-gel method in short time, low temperature and relatively simple way using simple equipments and investigation of structural properties and testing catalytic activity of  $\text{LaNiO}_3$  nanopowder. We have observed antibacterial activity of rhombohedral  $\text{LaNiO}_3$ . Formed mixed metal oxide shows good antibacterial activity for *S. aureus*. First time we are going to report antibacterial activity of  $\text{LaNiO}_3$  nanopowder.

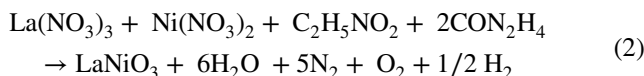
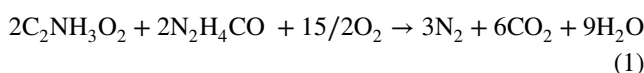
## Materials and methods

### Experimental

$\text{LaNiO}_3$  was prepared by sonicated sol-gel combustion method using glycine and urea as combination fuel. All

chemical reagents were of analytical grade and used without further purification. stoichiometric quantity of solid mixture of 100 ml of 0.1 M lanthanum nitrate  $\text{La}(\text{NO}_3)_3 \cdot 6\text{H}_2\text{O}$ , 100 ml of 0.1 M nickel hexahydrate  $\text{Ni}(\text{NO}_3)_2 \cdot 6\text{H}_2\text{O}$  (NN), 100 ml of 0.15 M of glycine, 100 ml of 0.15 M of urea were mixed well and sonicated at 5 Hz for 10 min at 60 °C. All solutions were mixed well with the help of magnetic stirrer and dried at 70–80 °C. Formed sol was heated at 175 °C for autocombustion on hot plate. At temperature 175 °C  $\text{LaNiO}_3$  powder was formed within 5 min. Surface area was measured by BET nitrogen gas adsorption method is 9.22  $\text{m}^2/\text{g}$ . Flow sheet diagram of formation of  $\text{LaNiO}_3$  is as shown in Fig. 2.

. heated at 175 °C reaction proceed by mechanism indicated by Eqs. 1 and 2 gives final products



## Results and discussion

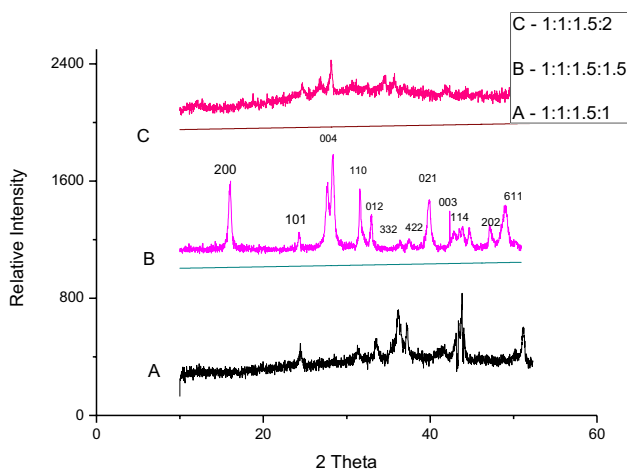
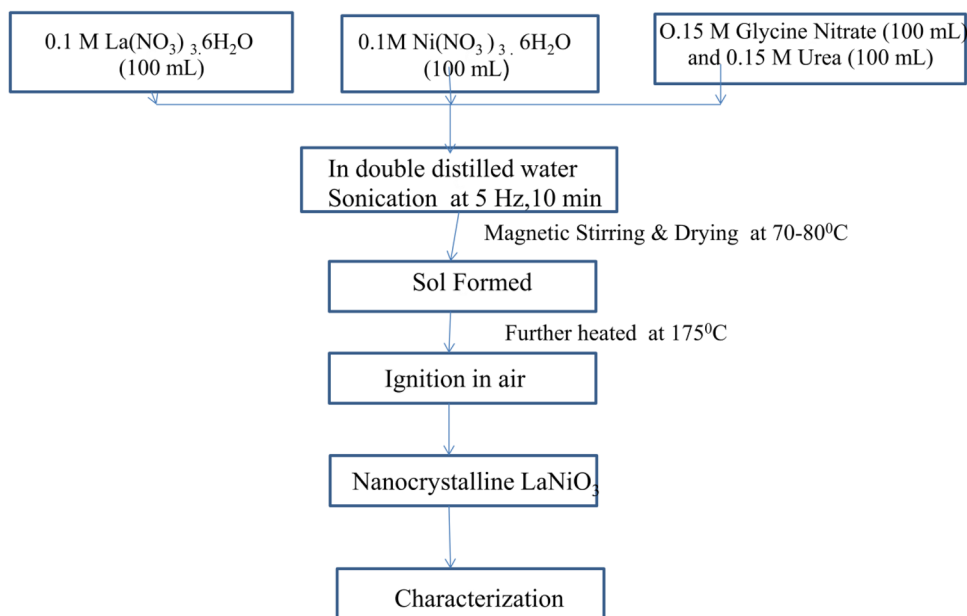
### XRD of $\text{LaNiO}_3$

XRD pattern of  $\text{LaNiO}_3$  is as shown in Fig. 3. All peaks indexed to rhombohedral structure and show matching with JCPDS card no (00-033-0711). Advanced X-ray diffraction using  $\text{Cu K}\alpha$  1.5456 radiation. Average crystallite size of formed  $\text{LaNiO}_3$  is calculated by using Scherrer's formula [26, 27] is 46 nm

$$t = 0.9\lambda / \beta \cos\theta, \quad (3)$$

where  $\lambda$  is wavelength of diffracted peaks and  $\theta$  is the angle of diffraction,  $t$  is average crystallite size. Average crystallite size was calculated by assuming particle to be spherical  $k = 0.9$ ,  $\beta$  is full width at half maximum and is integral breath that depend on width of most predominant peak. Rhombohedral  $\text{LaNiO}_3$  oxide have lattice parameters are  $a = b = 5.4570$  Å,  $c = 6.5720$  Å and  $\alpha = \beta = 90^\circ$   $\lambda = 120^\circ$ .

Different combinations of lanthanum nitrate, nickel nitrate, glycine and urea in proportion to 1:1:1.5:1, 1:1:1.5:1.5, 1:1:1.5:2 were studied. We obtained good result for 1:1:1.5:1.5 ratio of lanthanum nitrate hexahydrate  $\text{La}(\text{NO}_3)_3 \cdot 6\text{H}_2\text{O}$ (LN), nickel nitrate  $\text{Ni}(\text{NO}_3)_2 \cdot 6\text{H}_2\text{O}$ (NN), glycine and urea. Different scientist prepared  $\text{LaNiO}_3$ , they subject sample for annealing. We had prepared  $\text{LaNiO}_3$  by sonicated sol-gel method which did not required calcination. We have saved that energy which required for calcination, this showed green approach.

**Fig. 2** Flow sheet of preparation of  $\text{LaNiO}_3$ **Fig. 3** XRD patterns of  $\text{LaNiO}_3$ , (A) 1:1:1.5:1 ratio of lanthanum nitrate:nickel nitrate:glycine:urea, (B) 1:1:1.5:1.5 ratio of lanthanum nitrate:nickel nitrate:glycine:urea, (C) 1:1:1.5:2 ratio of lanthanum nitrate:nickel nitrate:glycine:urea

### SEM image Of $\text{LaNiO}_3$

To study morphology of formed oxide, scanning electron microscopy technique was used which revealed morphology and porous nature with particle size 45.33 nm.

SEM image of  $\text{LaNiO}_3$  powder prepared by sonicated sol-gel method using combination fuel at 175 °C is shown as in Fig. 4. To study scanning electron microscope image QUANTA 200 3D model was used. We can also observe macro agglomeration of very fine particles with size less than 1  $\mu\text{m}$ . Many small and large pores are observed on the surface of whole material. SEM images were captured at 1  $\mu\text{m}$ , 10  $\mu\text{m}$ , 500 nm.

### BET surface area of $\text{LaNiO}_3$

BET surface area of  $\text{LaNiO}_3$  was measured at 1100 °C by Flow BET Nitrogen Gas ISO S4652/ASTM D-3037/ USP846/EP 2.926 adsorption method is 9.22  $\text{m}^2/\text{g}$ . High surface area of formed rhombohedral  $\text{LaNiO}_3$  was obtained from BET measurements. Table 1 shows comparative study of surface area of  $\text{LaNiO}_3$  (Table 2).

From this study it is clear that large surface area is available for any chemical transformation, therefore  $\text{LaNiO}_3$  will show good catalytic activity. Sonicated sol-gel method provides high surface area metal oxide without calcination process. We have saved that energy used for calcination which reveals green approach. Sonication process shows creation of vacuume and small bubble which form homogeneous mixing of solution. Because of Sonication process change in physical as well as chemical properties of oxide takes place. Hydroxide soles shows critical nucleation process. Growth of particle size starts, after nucleation. Size of metal oxide regulated using sonication. Sonication barriers formation of aggregation of particles. Sonication involves breakage of intermolecular interactions and speed up dissolution. Use of mixed fuels like glycine and urea helps in vigorous combustion and produces nanoparticles.

### TG/TGA of $\text{LaNiO}_3$

TG curve shows little bit loss might be due to loss of moisture,  $\text{CO}_2$  and nitrogen, hydrogen gas as shown in Fig. 5. During preparation of rhombohedral  $\text{LaNiO}_3$  at 175 °C reaction proceeds by mechanism indicated by Eqs. 1 and 2



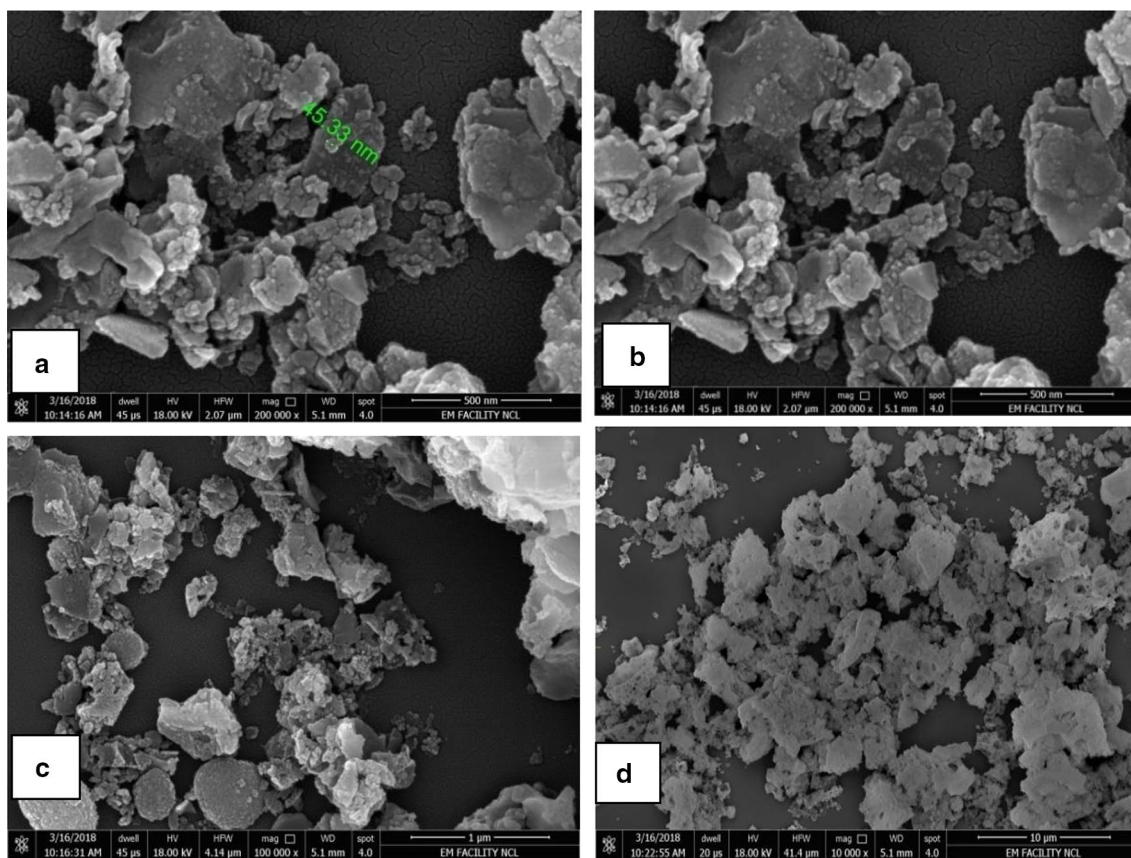


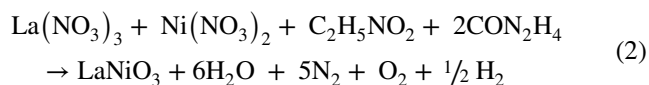
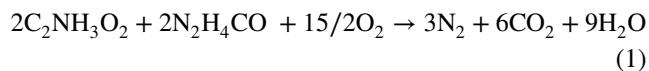
**Fig. 4** SEM image of  $\text{LaNiO}_3$  powder: **a** 500 nm, **b** 500 nm, **c** 1  $\mu\text{m}$  and **d** 10  $\mu\text{m}$

**Table 1** Comparative study of surface area of  $\text{LaNiO}_3$

Sr. No.	Method	Surface area $\text{LaNiO}_3$ ( $\text{m}^2/\text{g}$ )	References
1	Precipitation method at 900 °C	4.8	[28]
2	Citrate sol-gel method	3	[29]
3	Sol gel at 750 °C	9.1	[30]
	At 800 °C	7.5	
4	Pechini method	0.9	[31]
	EDTA cellulose method	2.6	
5	Modified citrate sol-gel method	5	[32]
6	Sonicated sol-gel combustion method	<b>9.22</b>	

**Table 2** Percentage composition of element

Element	Atomic No.	Series	Unn. [wt.%]
O	8	K	86.17
La	57	L	8.88
Ni	28	K	4.95
Total			100.00%



TG curve show formed oxide is very stable up to 900 °C as in Fig. 5.



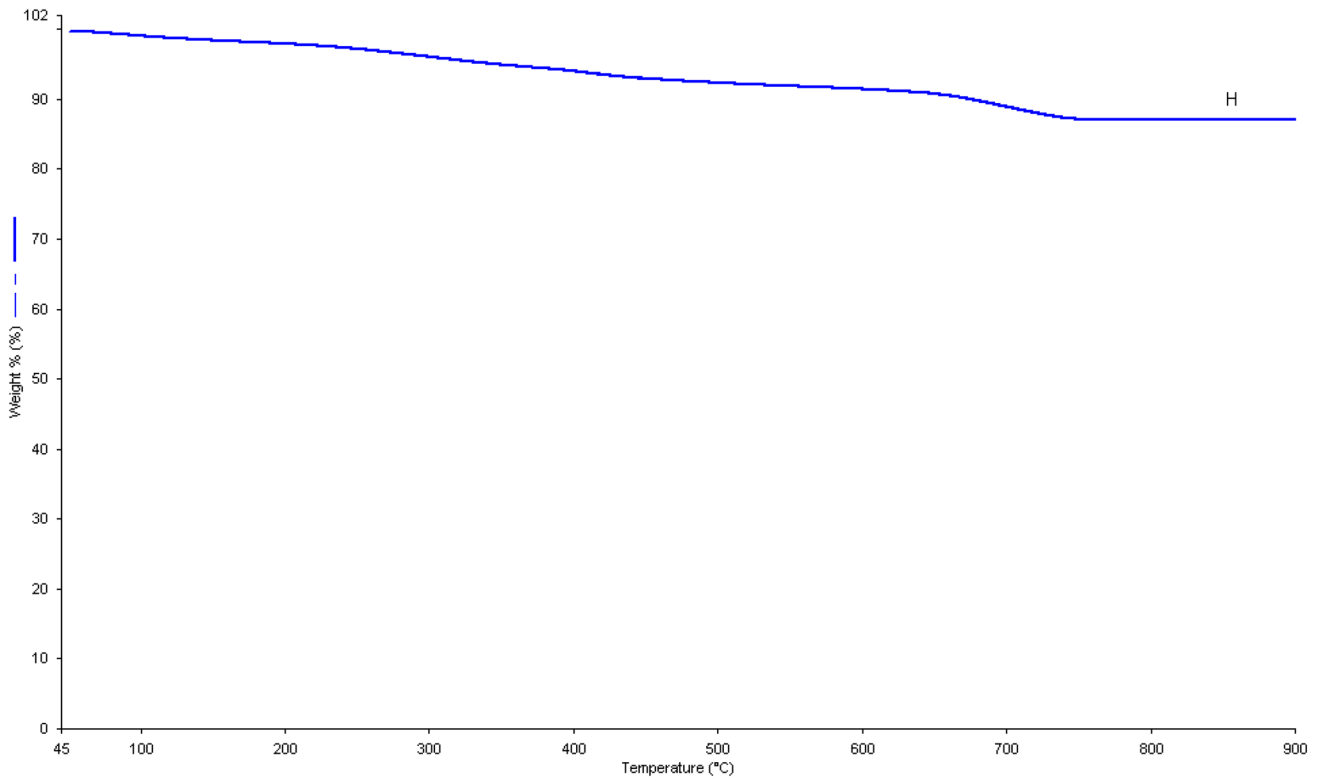


Fig. 5 TG curve of LaNiO<sub>3</sub> powder as prepared

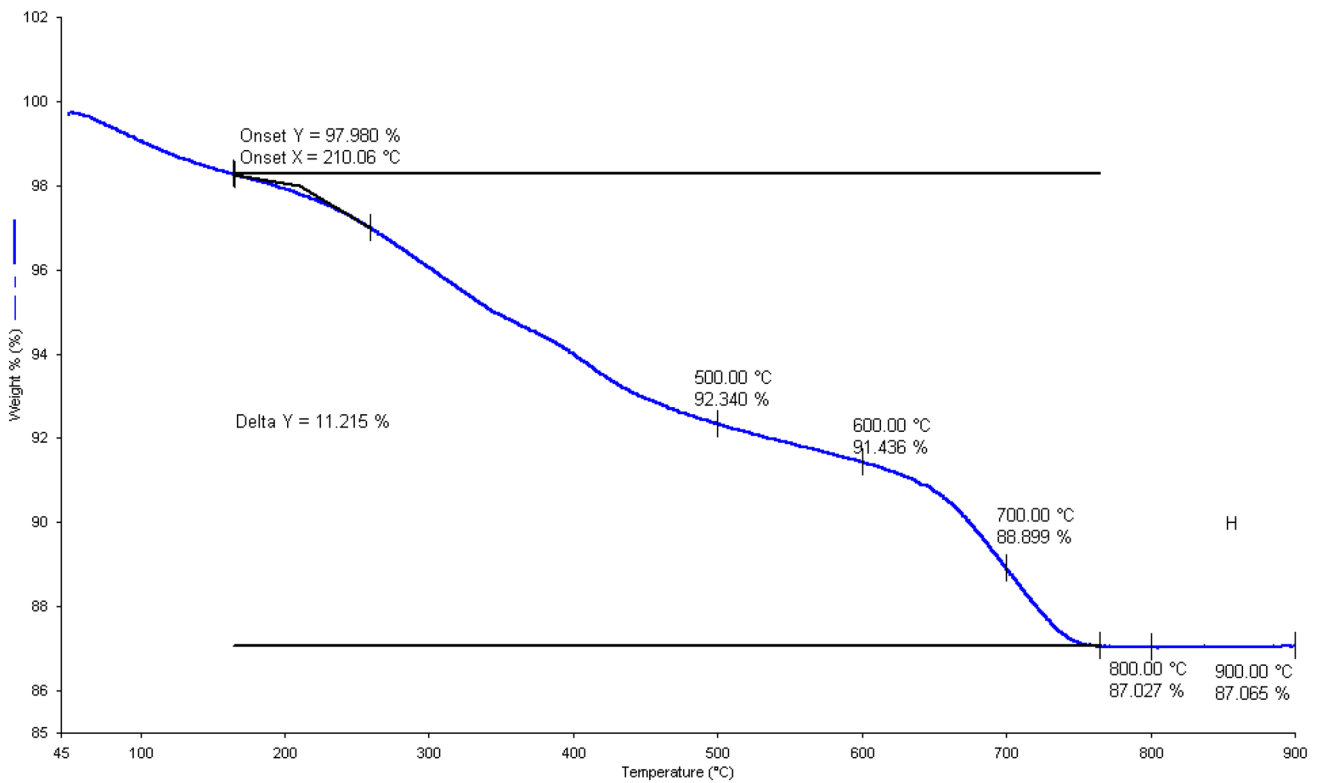


Fig. 6 TGA curve of LaNiO<sub>3</sub> powder as prepared

TGA show 11.21 % loss in weight from 210 °C to 800 °C which might be due to loss in moisture, nitrogen, CO<sub>2</sub> as in Fig. 6.

TGA is recorded in nitrogen gas by using Perkin and Elmer's STA 6000 is shown in Fig. 6. This weight loss and weight gain can be ignorable. This indicated that prepared powder was stable from bigining TGA curve show there is weight loss between 210 °C to 740 °C about 11.21 % which due to loss of moisture, CO<sub>2</sub> and nitrogen, hydrogen gas.

### EDX of LaNiO<sub>3</sub>

To study EDX of LaNiO<sub>3</sub> ELITE PLUS model is used. To study percentage composition of formed oxide, EDX was studied which show percentage of oxygen is 86.17 %, percentage of lanthanum is 8.88 %, percentage of nickel is 4.95 % as shown in Fig. 7.

EDX results clearly shows that formed LaNiO<sub>3</sub> contain only lanthanum, nickel, oxygen without any impurity.

## Antibacterial activity of LaNiO<sub>3</sub>

### Introduction

Use of mixed metal oxides as antibacterial agent has attracted scientist because of their reliable antimicrobial activity effective at low concentration. High surface area and small particle size of mixed metal oxides allows broad range of reaction with bacterial surface [33]. Metal oxides shows antibacterial activity against different gram positive and gram negative bacteria, as they are harmless to mammalian cells and environment also. Nanoparticles are found to be cytotoxic. As cytotoxic effect was size dependant, smaller particle size shows greater efficiency in inhibiting bacterial growth. Biofilm is community of bacteria implanted in self produced extracellular matrix of proteins, polysaccharides along with DNA. Infections which involve biofilm formation are chronic and cause serious damage to human beings. Hence it is major challenge to find alternative therapeutic way to overcome increasing resistance of bacteria to currently used common antibiotics. Use of

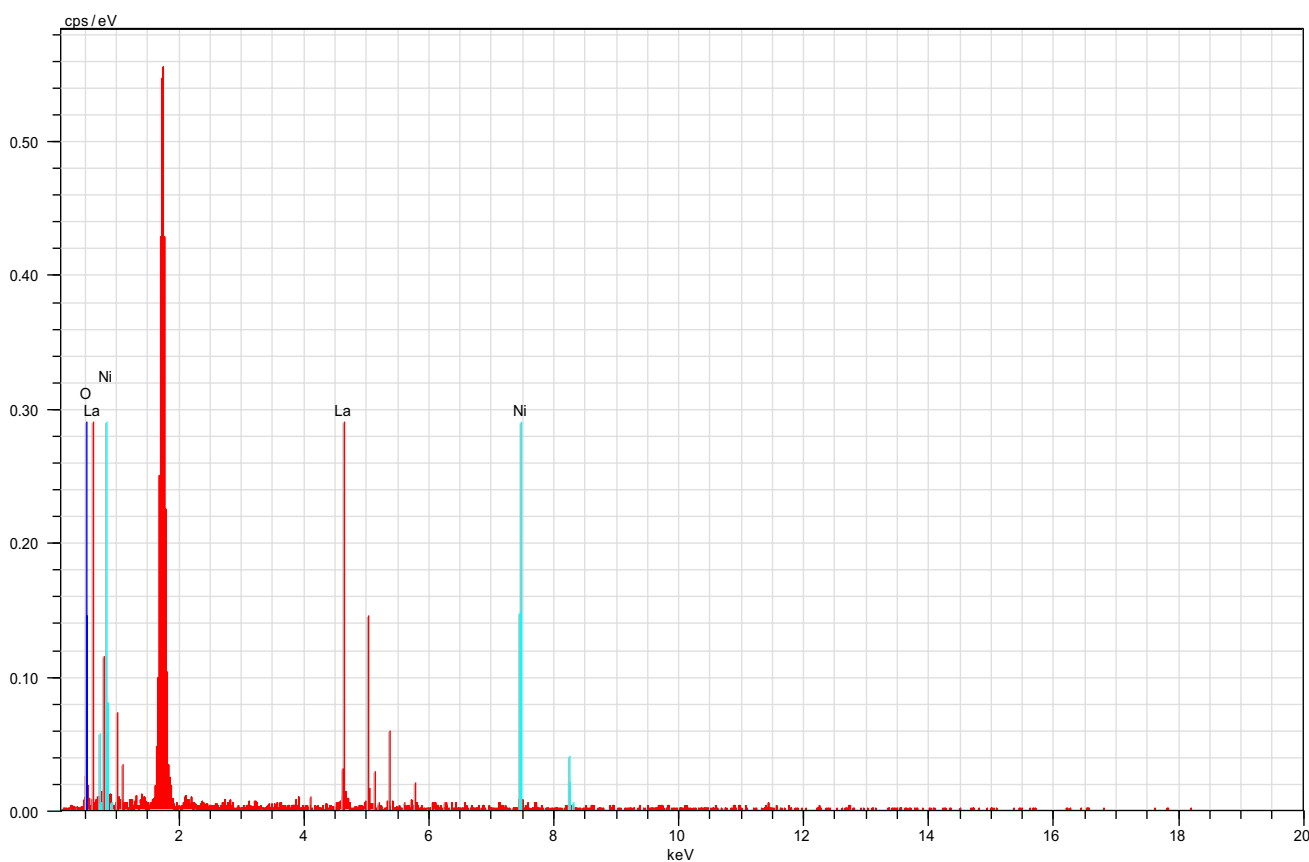


Fig. 7 EDX curve of LaNiO<sub>3</sub> powder as prepared



nanoparticles is found to be showing promising, good antibacterial activity. Although exact bactericidal mechanism of nanoparticles are still being investigated, different nanoparticles are found to be showing striking antimicrobial effects. Bacterial species shows selectivity for particular nanoparticles. Silver nanoparticles shows antibacterial activity efficiently than copper nanoparticles against *E. coli* and *S. aureus*, while *B. subtilis* shows more susceptibility to copper nanoparticles than silver nanoparticles [34]. Nanoparticles of titanium dioxide shows greater antibacterial activity against *E. coli* than *S. typhimurium*. Sensitivity and selectivity of bacteria to nanoparticles is related with species. Vancomycin-resistant bacteria like Enterococci found to develop additional outer membrane which covers cellular surface and provide protection to bacteria from vancomycin. Therefore vancomycin capped gold nanoparticles penetrate outer cell membrane, that allows vancomycin to ingress cellular surface [35]. Size of nanoparticles plays important role in its toxicity. Scientist studied effect of particle size on antibacterial efficiency. Hayden et al shows 2 nm gold nanoparticles are more toxic to *B. subtilis* than 6 nm gold nanoparticles [36]. Different types of metal and metal oxide nanoparticles like oxides of copper, silver, zinc, magnesium, gold, calcium shows antibacterial effect against wide varieties of various gram-negative and gram-positive bacteria [37]. Antibacterial activity of metal oxides are found to be effective against gram-negative bacteria *E. coli* and *P. aeruginosa* and gram-positive *S. aureus* and *B. subtilis* [38–41]. (Fig. 8)

*Staphylococcus aureus* is a gram-positive bacteria with round shape belongs to family Firmicutes. They able to grow without oxygen [42]. They are opportunistic pathogen produces skin infection, abscesses, respiratory infection,

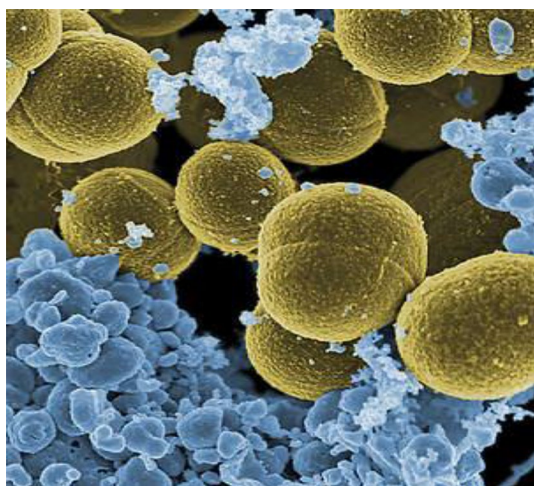


Fig. 8 Image of *Staphylococcus aureus* bacteria

sinusitis, food poisoning. Pathogen strains promote infections by production of virulence factors.

### Results and discussion

Antibacterial activity of rhombohedral  $\text{LaNiO}_3$  nanocatalyst was studied for *E. coli*, *S. aureus*, *Streptococcus* spp., *P. aeruginosa*, *B. subtilis* and antifungal activity for *C. albicans*. Zone of inhibition of 13 mm for antibacterial activity was

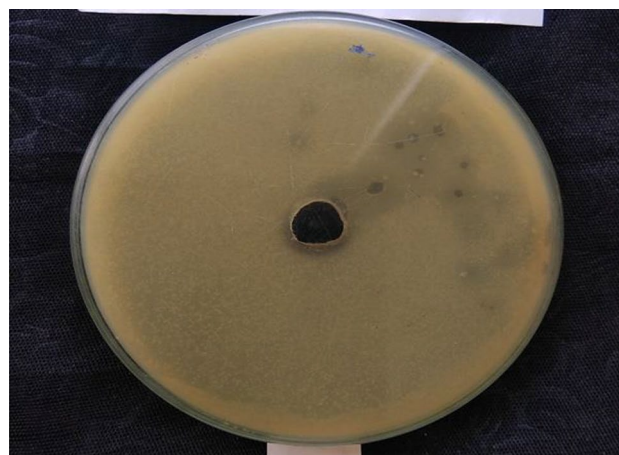


Fig. 9 Antibacterial activity of  $\text{LaNiO}_3$  *Staphylococcus aureus* bacteria

Table 3 Antibacterial activity of  $\text{LaNiO}_3$

Catalyst	$\text{LaNiO}_3$
( <i>Staphylococcus aureus</i> )	13 mm
( <i>Pseudomonas</i> bacteria)	Inactive
<i>Escherichia coli</i>	Inactive
<i>Streptococcus</i> spp.	Inactive
<i>Bacillus subtilis</i>	Inactive
<i>Candida albicans</i>	Inactive

Table 4 Zone of inhibition of antibiotics for *Staphylococcus aureus*

Name of antibiotic	Zone of inhibition (mm)
Oxacillin 1 $\mu\text{g}$	13
Cefotaxime 30 $\mu\text{g}$	19
Amikacin 30 $\mu\text{g}$	17
Ciprofloxacin 5 $\mu\text{g}$	21
Vancomycin 30 $\mu\text{g}$ [43]	13
<i>B. oleracea</i> methanol extract 500 mg [44]	11.5
<i>Curcuma longa</i> rhizome extract 100 mg [45]	12

**Table 5** Toxicity of LaNiO<sub>3</sub>

Sr. No.	Extract in	Concentration (µg/mL)	Total shrimps taken for study	Number of shrimps survived	Number of shrimps dead	Percentage of death inhibition (%)
1	Water	10	10	10	0	0.00
2		50	10	8	2	20.00
3		500	10	8	2	20.00

observed for *S. aureus* as shown in Fig. 9. It was inactive against antifungal activity for *C. albicans*.

Though exact mechanism of antibacterial activity of rhombohedral LaNiO<sub>3</sub> nanocatalyst was not known, it was believed that rhombohedral LaNiO<sub>3</sub> catalyst shows antibacterial activity through ion diffusion. We here going to report antibacterial activity of rhombohedral LaNiO<sub>3</sub> for *S. aureus* with good results.

As shown in Table 3 we also study antibacterial activity for *E. coli*, *Streptococcus* spp., *B. subtilis* and antifungal activity *C. albicans*. LaNiO<sub>3</sub> do not shows antibacterial activity for *E. coli*, *Streptococcus* spp., *B. subtilis* and antifungal activity for *C. albicans* (Table 4).

### Cytotoxicity of LaNiO<sub>3</sub>

LaNiO<sub>3</sub> is nontoxic at low concentration. Toxicity of LaNiO<sub>3</sub> was studied in water extract. Brine Shrimps Lethality Assay Method was used to study cytotoxicity of LaNiO<sub>3</sub>. It was found that LaNiO<sub>3</sub> was non-toxic at 10 µg/ml in water and at high concentration 500 µg/ml its toxicity is 20 % as shown in Table 5.

### Summary

LaNiO<sub>3</sub> nanocatalyst was prepared by using sonicated sol-gel method. The precursors used in this method were lanthanum nitrate hexahydrate La(NO<sub>3</sub>)<sub>3</sub>·6H<sub>2</sub>O(LN), nickel nitrate Ni(NO<sub>3</sub>)<sub>3</sub>·6H<sub>2</sub>O(NN), glycine and urea as combination fuel. Sonication was carried out at 5 Hz for 10 min. After autocombution at 175 °C LaNiO<sub>3</sub> was formed. Formed nanomaterial was characterized with the help of XRD, TGA, SEM, IR, BET surface area, EDX. Particle size of LaMnO<sub>3</sub> was determined by Debye Scherrer's equation and was found to be 48 nm. Surface area of nanomaterial was 9.22 m<sup>2</sup>/g, which was high as compared to other researchers. LaNiO<sub>3</sub> nanocatalyst was used to study antibacterial activity. We have reported first time good antibacterial activity of LaNiO<sub>3</sub> for *S. aureus*. Zone of inhibition for *S. aureus* of LaNiO<sub>3</sub> was 13 mm which was studied with the help of agar cup method.

### Conclusion

We have successfully prepared rhombohedral LaNiO<sub>3</sub> catalyst by sonicated sol-gel method in short time with good surface area, using simple equipments in good yield and reactivity. Prepared LaNiO<sub>3</sub> nanocatalyst characterized by XRD, SEM, TG, BET, EDX which shows formed oxide was rhombohedral with size 45.33 nm. Surface area of LaNiO<sub>3</sub> was 9.22 m<sup>2</sup>/g. We have reported first time antibacterial activity of LaNiO<sub>3</sub> against *S. aureus* in good extent.

**Acknowledgements** We are thankful to National Chemical Laboratory, Pune; Department of Chemistry and Department of Physics, Shivaji University Kolhapur; S.P.Consultant Mumbai, Department of Chemistry, Dahiwadi College Dahiwadi for valuable assistance in data collection. I am also thankful to Pavan Dongapure for their guidance.

**Funding** None.

### Compliance with ethical standards

**Conflict of interest** We have no Conflict of interest

**Open Access** This article is distributed under the terms of the Creative Commons Attribution 4.0 International License (<http://creativecommons.org/licenses/by/4.0/>), which permits unrestricted use, distribution, and reproduction in any medium, provided you give appropriate credit to the original author(s) and the source, provide a link to the Creative Commons license, and indicate if changes were made.

### References

1. Das, A.K., Divya, A.M., Pareek, S.V.: One-step green synthesis and characterization of plant protein-coated mercuric oxide (HgO) nanoparticles: antimicrobial studies, *Int. Nanolett.* **5**(3), 125–132 (2015)
2. Nam, G., Purushothaman, B., Rangasamy, S.: Investigating the versatility of multifunctional silver nanoparticles: preparation and inspection of their potential as wound treatment agents. *Int. Nanolett.* **6**(1), 51–63 (2016)
3. Lindsay: Genomic variation and evolution of *Staphylococcus aureus*, *J. Int. J. Med. Microbiol.*, **300**(2–3), 98 (2010)
4. Fitzgerald, J.R.: Evolution of *Staphylococcus aureus* during human colonization and infection. *Infect. Genet. Evol.* **21**, 542–547 (2014)
5. Arciola, C.R., Campoccia, D., Speziale, P., Montanaro, L., Costerton, J.W.: Biofilm formation in *Staphylococcus* implant infections. A review of molecular mechanisms and implications for biofilm-resistant materials. *Biomaterials.* **33**(26), 5967–5982 (2012)

6. Fuente-Nunez, C., Reffuveille, F., Fernandez, L., Hancock, R.E.: Bacterial biofilm development as a multicellular adaptation: antibiotic resistance and new therapeutic strategies. *Curr. Opin. Microbiol.* **16**(5), 580–589 (2013)
7. de Lima, S.M., Assaf, J.M.: Synthesis and characterization of  $\text{LaNiO}_3$ ,  $\text{LaNi}(1-x)\text{Fe}_x\text{O}_3$  and  $\text{LaNi}(1-x)\text{Co}_x\text{O}_3$  perovskite oxides for catalysis application. *J. Mat. Res.* **5**(3), 329–335 (2002)
8. Choudhary, V.R., Uphade, B.S., Belhekar, A.A.: Oxidative conversion of methane to syngas over  $\text{LaNiO}_3$  perovskite with or without simultaneous steam and  $\text{CO}_2$  reforming reactions: influence of partial substitution of La and Ni. *J. Catal.* **163**(2), 312–318 (1996)
9. Levy, P., Leyva, A.G., Troiani, H.E.: Nanotubes of rare-earth manganese oxide. *J. Appl. Phys. Lett.* **83**, 5247–5249 (2003)
10. Tagliazucchi, M., Sanchez, R.D., Troiani, H.E., Calvo, E.J.: Synthesis of lanthanum nickelate perovskite nanotubes by using a template-inorganic precursor. *Solid State Commun.* **137**, 212–215 (2006)
11. Fernandes, J.D.G., Melo D.M.A., Zinner, L.B.: Low-temperature synthesis of single-phase crystalline  $\text{LaNiO}_3$  perovskite via Pechini method. *Mater. Lett.* **53**, 122 (2002)
12. Chawl, S.K., Milka, G., Patel, F., Patel, S.: Production of synthesis gas by carbon dioxide reforming of methane over nickel based and perovskite catalysts. *Proc. Eng.* **51**, 461–466 (2013)
13. Pechini, M.: US Patent 3231328 (1966)
14. Goodenough, J.B.: Interpretation of the transport properties of  $\text{Ln}_2\text{NiO}_4$  and  $\text{Ln}_2\text{CuO}_4$  compounds. *Mater. Res. Bull.* **8**, 423 (1973)
15. Tagliazucchi, Mario, Sanchez, Rodolfo D., Troiani, Horacio E.: Synthesis of lanthanum nickelate perovskite nanotubes by using a template-inorganic precursor. *Solid State Communications* **137**, 212–215 (2006)
16. Moradi, P., Patvari, M., Irani, J.: Preparation of lanthanum–nickel–aluminium perovskites system and their application in methane reforming reactions. *Iran. J. Chem. Eng.* **3**(3) (2006)
17. Gallego, G.S., Mondragon, F.: Dry reforming of methane over  $\text{LaNi}_{1-y}\text{B}_y\text{O}_{3\pm\delta}$  ( $\text{B} = \text{Mg}, \text{Co}$ ) perovskites used as catalyst precursor. *J. Appl. Catal. A* **334**, 251–258 (2008)
18. Khaledi, A., Parvari, M.: Dry reforming of methane on modified perovskite catalysts, Department of Chemical Engineering, Iran University of Science and Technology, Tehran, Iran
19. Gallego, G.S., Mondragon, F.:  $\text{CO}_2$  reforming of  $\text{CH}_4$  over La–Ni based perovskite precursors. *J. Appl. Catal. A* **311**, 164–171 (2006)
20. Rivas, M.E., Fierro, J.L.G., Goldwasser, M.R., Pietri, E., Perez-Zurita, M.J., Griboval-Constant, A., Leclercq, G.: Structural features and performance of  $\text{LaNi}_{1-x}\text{Rh}_x\text{O}_3$  system for the dry reforming of methane. *Appl. Catal. A*, **344**, 10–19 (2008)
21. El Rhazi, M., Majid, S., Elbasri, M., Ezzahra, F.: Recent progress in nanocomposites based on conducting polymer: application as electrochemical sensors. *Int. Nanolett.* **8**(2), 79–99 (2018)
22. Uddin, M.J., Islam, Md.A., Ariful, S.: Preparation of nanostructured  $\text{TiO}_2$ -based photocatalyst by controlling the calcining temperature and pH. *Int. Nanolett.* **2**, 19 (2012)
23. Cassir, M., Chavez Guerrero, L.: Synthesis, characterization of  $\text{LaNi}_x\text{Co}_{1-x}\text{O}_3$  Role of microstructure on magnetic properties. *J. Rare Earths* **33**(3), 277 (2015)
24. Rida, K., Pena, M.A., Sastre, E.: Effect of calcination temperature on structural properties and catalytic activity in oxidation reactions of  $\text{LaNiO}_3$  perovskite prepared by Pechini method. *J. Rare Earths* **30**(3), 210–221 (2012)
25. Hsiao, C.-L., Chang, W., Qi, X.: Sol-gel synthesis and characterisation of nanostructured  $\text{LaNiO}_{3-x}$  for thermoelectric applications. *Sci. Adv. Mater.* **6**(7) (2013)
26. Cullity, B.D.: Element of X-ray diffraction, vol. 99. Addison-Wesley, London (1956)
27. Khetre, S.M., Bamane, S.R.: synthesis and characterization of nanocrystalline  $\text{LaNiO}_3$  by combustion route. *Rasayan J. Chem.* **2**(1), 174–178 (2009)
28. de Lima, S.M., Assaf, J.M.: Synthesis and characterization of  $\text{LaNiO}_3$ ,  $\text{LaNi}(1-x)\text{Fe}_x\text{O}_3$  and  $\text{LaNi}(1-x)\text{Co}_x\text{O}_3$  perovskite oxides for catalysis application. *J. Mat. Res.* **5**(3), 329 (2002)
29. Talaie, N., Sadr, M.H.: Synthesis and application of  $\text{LaNiO}_3$  perovskite-type nanocatalyst with Zr for carbon dioxide reforming of methane orient. *J. Chem.* **32**(5) (2016)
30. Huynh, K.-N., Pham, K.O.: Photocatalytic activity of lanthanum nickelate under simulated visible-light irradiation. *J. Sci. Eng. Res.* **4**(3), 95–101 (2017)
31. Yanga, E.-h., Moon, D.J., Synthesis of  $\text{LaNiO}_3$  perovskite using an EDTA-cellulose method and comparison with the conventional Pechini method: application to steam  $\text{CO}_2$  reforming of methane. *RSC Adv.* **114**, 112885–112898 (2016)
32. Jahangiri, A., Pahlavanzadeh, H., Synthesis, characterization and catalytic study of Sm doped  $\text{LaNiO}_3$  nanoparticles in reforming of methane with  $\text{CO}_2$  and  $\text{O}_2$ . *Int. J. Hydrogen Energy.* **37**, 9977–9984 (2012)
33. Nelson, D.L., Cox, M.M.: Lehninger Principles of Biochemistry **5**, 183–229 (2008)
34. Ragg, R., Tahir, M.N., Tremel, W.: Solids go bio: inorganic nanoparticles as enzyme mimics. *Eur. J. Inorg. Chem.* 1906–1915 (2016)
35. Wang, X., Hu, Y., Wei, H.: Nanozymes in bionanotechnology: from sensing to therapeutics and beyond. *Inorg. Chem. Front.* **3**, 41–60 (2016)
36. Liu, B., Liu, J.: Surface modification of nanozymes. *Nano Res.* **10**, 1125–1148 (2017)
37. Manea, F., Houillon, F.B., Scrimin, P.: Nanozymes: gold-nanoparticle-based transphosphorylation catalysts. *Angew. Chem. Int. Ed.* **43**, 6165–6169 (2004)
38. Gao, L., Zhuang, J., Zhang, Y., Gu, N. et al.: Intrinsic peroxidase-like activity of ferromagnetic nanoparticles. *Nat. Nanotechnol.* **2**, 577–583 (2007)
39. Song, Y., Qu, K., Zhao, C., Ren, J., Qu, X.: Graphene oxide: intrinsic peroxidase catalytic activity. *Adv Mater.* **22**, 2206–2210 (2010)
40. Natalio, F., Hartog, A.F., Stoll, B., Jochum, K.P.: Vanadium pentoxide nanoparticles mimic vanadium haloperoxidases and thwart biofilm formation. *Nat. Nanotechnol.* **7**, 530 (2012)
41. Xia, X., Zhang, J., Lu, N., Kim, M.J., Ghale, K.: Pd–Ir core-shell nanocubes: a type of highly efficient and versatile peroxidase mimic. *ACS Nano* **9**, 9994–10004 (2015)
42. Masalha, M., Borovok, I., Schreiber, R., Aharonowitz, Y., Cohen, G.: Analysis of transcription of *Staphylococcus aureus* aerobic class Ib and anaerobic class III ribonucleotide reductase genes in response to oxygen. *J. Bacteriol.* **183**(24), 7260–7272 (2001)
43. Singh, R., Ray, P., Das, A., Sharma, M.: Penetration of antibiotics through *Staphylococcus aureus* and *Staphylococcus epidermidis* biofilms. *J. Antimicrob. Chemother.* **65**, 1955–1958 (2010)
44. Hafidh, R.R., Abdulmir, A.S.: Inhibition of growth of highly resistant bacterial and fungal pathogens by a natural product. *Open Microbiol.* **5**, 96–106 (2011)
45. Gupta, A., Mahajan, S., Sharma, R.: Evaluation of antimicrobial activity of Curcuma longa rhizome extract against *Staphylococcus aureus*. *Biotechnol. Rep.* **6**, 51–55 (2015)

**Publisher's Note** Springer Nature remains neutral with regard to jurisdictional claims in published maps and institutional affiliations.

